Noname manuscript No.
(will be inserted by the editor)

Calibration via multi-period state estimation in water distribution systems

Sarai Díaz · Roberto Mínguez · Javier González

The final publication is available at Springer via http://dx.doi.org/10.1007/s11269-017-1779-2

Abstract Calibration of model parameters is of utmost importance to ensure the good performance of hydraulic simulation models. In this work, calibration is conceived within a joint multi-period parameter and state estimation approach, where model parameters (i.e. roughness coefficients) and hydraulic variables should be computed from available measurements at different times. The aim of this paper is twofold: (1) to present a novel methodology for the calibration of water networks via multi-period state estimation, and (2) to adapt observability analysis to this approach. The novelty of this work is that such a large-scale non-linear optimisation problem is here solved using mathematical programming decomposition techniques. On the other hand, observability analysis requires the construction of the multi-period measurement and parameter Jacobian matrix of the problem. The proposed approach enables computation of the observable roughness coefficients from available readings over time, making possible the periodic reassessment of roughness values based on recent online measurements. The potential of the method is illustrated by means of a case study, which shows how such a methodology would contribute to make the most of telemetry data for calibration purposes.

Sarai Díaz
Dept. of Civil Eng., Univ. of Castilla-La Mancha, Av. Camilo José Cela s/n, 13071 Ciudad Real (Spain)
Tel.: +34 926295300 (Ext. 96635)
ORCID: orcid.org/0000-0002-5478-1768
E-mail: Sarai.Diaz@uclm.es

Roberto Mínguez
HIDRALAB INGENIERÍA Y DESARROLLOS, S.L., Spin-Off UCLM, Hydraulics Laboratory Univ. of Castilla-La Mancha, Av. Pedriza, Camino Moledores s/n, 13071 Ciudad Real (Spain)
E-mail: roberto.minguez@hidralab.com

Javier González
Dept. of Civil Eng., Univ. of Castilla-La Mancha, Av. Camilo José Cela s/n, 13071 Ciudad Real (Spain). //
HIDRALAB INGENIERÍA Y DESARROLLOS, S.L., Spin-Off UCLM, Hydraulics Laboratory Univ. of Castilla-La Mancha, Av. Pedriza, Camino Moledores s/n, 13071 Ciudad Real (Spain)
E-mail: Javier.Gonzalez@uclm.es

Keywords Weighted least squares · Decomposition techniques · Observability analysis · Network monitoring

1 Introduction

Hydraulic models are frequently used to simulate how a given water distribution system would work under specific circumstances, i.e. enabling different scenarios to be tested. For this reason, they have become an essential tool for both practitioners and researchers. In the industry domain, they are normally used to simulate different scenarios, based on which the understanding of the system can be furthered and decisions can be made to improve the network operation and enhance serviceability. In academia, they constitute the basis on which other related applications lay their foundation. Such is the case of algorithms for the efficient design of water systems, leakage detection strategies, optimal pump and valve operation, state estimation techniques, and other online monitoring and control applications. Nevertheless, all these applications rely on the fact that the simulation model accurately represents the actual system. Accordingly, it is a matter of utmost importance to correctly adjust model parameters using the available measurements in the network.

Numerous approaches have been presented in the past to solve the calibration problem, also known as the inverse problem. Savic et al (2009) classify calibration procedures in three categories: (1) iterative or trial-and-error methods, (2) explicit or hydraulic simulation procedures, and (3) implicit or optimisation models. Trial-and-error methods are ad hoc procedures that iteratively update model parameters based on the solution of the flow network, either considering a single demand scenario (Rahal et al, 1980) or multiple loading conditions (Bhave, 1988), with the latter being more robust as it permits to adjust the model based on different flow scenarios. In explicit approaches, model parameters are obtained by solving the extended system of steady-state equations that results from considering continuity and energy equations, together with the additional equations that can be derived from available measurements. Such methods are limited to even-determined systems of equations and may consider single (Boulos and Wood, 1990) or multiple (Boulos and Ormsbee, 1991) loading conditions. Implicit methods tackle the calibration problem with a weighted least squares (WLS) approach that minimises the difference between the metered or observed values and the estimated variables, which take into account the model parameters through the optimisation constraints, i.e. the flow governing equations. These procedures traditionally consider multiple loading conditions and have been solved in many different ways: applying the gradient method (e.g. Lansey and Basnet (1991)), sensitivity analysis techniques (e.g. Datta and Sridharan (1994)), Gauss-Newton based methods (e.g. Reddy et al (1996)) and genetic algorithms (e.g. Savic and Walters (1995), Kapelan et al (2007), Wu and Clark (2009)), among others. It should be noted that the aforementioned methodologies do not all consider the same calibration parameters. Roughness coefficients, nodal demands, pump and valve settings, leak coefficients or a combination of these have been considered as calibration parameters in the past (see Savic et al (2009) for details).

Such variety of approaches proves that calibration has been a matter of crucial interest in the water supply field since the 1970s. Nevertheless, there is not an ultimate solution to the problem yet, and calibration is still a topic of ongoing research (Savic et al, 2009). As recently pointed out by Kumar et al (2010), the majority of existing calibration procedures use a hydraulic model as the basis or engine for parameter adjustment, and do not consider the hydraulic state of the network using a "formal state estimation approach". The traditional view is that water levels at source nodes and water outflows are known (hence the hydraulic model works straightforwardly) and only additional measurements of pressure or flow are used to estimate model parameters (Lansey et al, 2001). However, in practice all measurements can sporadically fail (e.g. sensor failure, communication failure) and are subjected to noise, and that should be taken into account in the calibration process. To consistently simulate this reality, parameter estimation can be integrated with state estimation techniques.

A state estimator is an algorithm that provides the most likely hydraulic state of a water distribution system based on the available measurements, considering that model parameters are already known (Díaz et al, 2016). Some work has been done in the past at a scientific level to develop joint state and parameter estimation algorithms in static and dynamic water supply systems with bounded uncertainty (Brdys and Chen, 1993, 1994; Brdys and Ulanicki, 2002). More recently, Kumar et al (2010) have resumed the combined state and parameter estimation problem by simplifying the associated large-scale non-linear optimisation problem using graph theoretic principles (Kumar et al, 2008), but only for a single loading condition. It must be highlighted that considering multiple loading conditions leads to a significant increase in the size of the optimisation problem, as not only model parameters but also hydraulic variables at all loading conditions must be inferred from the available measurements. This fact complicates the use of real-time measurements provided by recently installed supervisory control and data acquisition (SCADA) systems for calibration purposes.

In this context, the aim of this paper is twofold: (1) to present a novel methodology for the calibration of water networks via multi-period state estimation, and (2) to assess the system observability for such calibration procedure. The calibration problem set out in this work results in a large-scale non-linear mathematical programming problem whose resolution poses new challenges from the computational perspective. The novelty of this paper is that we take advantage of mathematical programming decomposition techniques (Conejo et al, 2006) to tackle this difficulty. Hence, we decompose the original problem into a set of state estimation *subproblems* of substantially reduced complexity and a calibration problem, so called *master* problem. With that aim we consider calibration parameters as complicating variables, i.e. variables that if fixed to given values render a decomposable problem consisting on different state estimation problems at different times, which allows the evaluation of the objective function for given values of calibration parameters. In addition and using sensitivity analysis, derivatives of those objective functions with respect to calibration parameters are computed. Thus, the calibration or master problem reduces to an unconstrained non-linear mathematical programming problem, which depends on roughness coefficients (taken as calibration parameters in this work) and can be solved using Gauss-Newton type algorithms that only use first-order derivatives. This

enables the use of the telemetry data at different times for calibration purposes. The price to be paid for such advantage is the need of an iterative algorithm. On the other hand, observability analysis enables beforehand identification of which roughness coefficients could be adjusted based on the existing measurements over time.

The paper is organised as follows: firstly, the novel methodology for calibration of water distribution systems via multi-period state estimation is presented, including a detailed description of the decomposition technique adopted to simplify the joint parameter and state estimation inverse problem. Then, a strategy for observability analysis is provided for the aforementioned calibration procedure. This section includes an explanation of how the multi-period measurement and parameter Jacobian matrix must be built for this approach, as well as a brief presentation of how to assess observability from there. Subsequently, a case study is presented to show the potential and effectiveness of the methodology proposed in this paper when considering a different number of roughness parameters, and finally, conclusions are concisely drawn.

2 Calibration via multi-period state estimation

2.1 General approach

The calibration problem is conceived in this work starting from a joint multi-period parameter and state estimation approach. To begin with, the set of state variables, i.e. the minimum set of variables needed to compute the hydraulic state of the system based on the hydraulic governing equations (Brdys and Ulanicki, 2002), for such problem must be defined. Note that for a conventional state estimation process, head levels can be taken as state variables on their own, as any combination of nodal heads can determine the hydraulic state of the system (Díaz et al, 2016). For the joint parameter and state estimation problem, model parameters must also be included as state variables. More specifically, pipe roughness coefficients (Hazen-Williams constants) are considered the only model parameters in this paper, as done before by Savic and Walters (1995), Kapelan et al (2007) and Kumar et al (2010), among others. According to this selection, there are as many state variables as the number of nodes in the network (n) multiplied by the number of times considered (n_t), and plus the number of roughness coefficients (p). Note that roughness coefficients can be assumed constant in time for a reasonable time period, but measurements, and thus head levels, are different for each loading condition or time step t.

The joint multi-period parameter and state estimation problem can then be posed as the following non-linear WLS mathematical programming problem:

$$\underset{\boldsymbol{x_t};\forall t,\boldsymbol{C}}{\text{Min}}\, J = \sum_{\forall t} J_t\left(\boldsymbol{x_t}, \boldsymbol{z_t}, \boldsymbol{C}\right) = \sum_{\forall t} \frac{1}{2}\left[\boldsymbol{z_t} - \boldsymbol{h_t}(\boldsymbol{x_t}, \boldsymbol{C})\right]^T \boldsymbol{R}_{\boldsymbol{z_t}}^{-1}\left[\boldsymbol{z_t} - \boldsymbol{h_t}(\boldsymbol{x_t}, \boldsymbol{C})\right] \tag{1}$$

subject to

$$\boldsymbol{l_t}(\boldsymbol{x_t}, \boldsymbol{C}) = \boldsymbol{0};\, \forall t = 1, 2, \ldots, n_t \tag{2}$$

$$\boldsymbol{g_t}(\boldsymbol{x_t}, \boldsymbol{C}) \leq \boldsymbol{0};\, \forall t = 1, 2, \ldots, n_t, \tag{3}$$

where $\hat{\boldsymbol{x}}_{\boldsymbol{t}}; \forall t = 1, 2, \ldots, n_t$ and $\hat{\boldsymbol{C}}$ represent the optimal solution of the problem and $\hat{J}$ the optimal objective function. Note that $\boldsymbol{x_t} \in \mathbb{R}^n$ and $\boldsymbol{z_t} \in \mathbb{R}^m$ represent the head level and measurement vectors for each time t, respectively, and $\boldsymbol{C} \in \mathbb{R}^p$ is the roughness coefficient vector, which remains constant for the considered times or loading conditions. Moreover, $\boldsymbol{h_t} : \mathbb{R}^n, \mathbb{R}^p \rightarrow \mathbb{R}^m$ is the non-linear relationship between measurements and estimates at each time, and $\boldsymbol{R}_{\boldsymbol{z_t}}^{-1}$ is the measurement variance-covariance matrix at time t, calculated as the inverse of the weight matrix. On the other hand, Eqs. (2)-(3) represent the hydraulic constraints of the problem for each time, which include mass balance and energy equations. Note that pseudo-static state estimation is considered in this work all along, as the state estimation from each loading condition or measurement set corresponds to an independent instantaneous snapshot of the network (Díaz et al, 2016), i.e. no relationship needs to exist between different loading conditions or time steps.

It should be noted that, as mentioned in the Introduction, the number of variables ($n \times n_t + p$) of the multi-period state estimation problem (1)-(3) considerably increases as the number of loading conditions enlarges. This constitutes a major limitation for the use of the SCADA systems for calibration purposes, even if grouping strategies are used to reduce the number of roughness coefficients (Kumar et al, 2010). Such platforms provide readings from metering devices in subsequent times, which could be understood as different loading conditions that provide first-hand real-time information about the state of the system, i.e. they are a good reference for calibration. Nevertheless, optimisation problem (1)-(3) needs to be simplified somehow in order to be suitable to estimate roughness coefficients considering multi-period information.

2.2 Decomposition technique

As the purpose of this work is to provide a novel methodology for calibration of water distribution systems based on available measurements over time rather than solving directly the joint parameter and state estimation issue, problem (1)-(3) can be decomposed into a set of state estimation *subproblems* of substantially reduced complexity and a calibration problem, so called *master* problem. With that aim we consider roughness coefficients as complicating variables, i.e. variables that if fixed to given values render a decomposable problem consisting on different state estimation problems at different times, which allows the evaluation of the objective function for given values of calibration parameters. Note that if roughness coefficients are fixed to given values instead of being considered unknowns, the multi-period state estimation problem could be easily solved, providing the head levels at each time $\hat{\boldsymbol{x}}_{\boldsymbol{t}}$ from each of the independent available measurement sets $\boldsymbol{z_t}$.

Therefore, problem (1)-(3) can be decomposed by firstly considering a battery of n_t subproblems where $\boldsymbol{C}$ is a given particular value $\boldsymbol{C}^{(k)}$:

$$\hat{\boldsymbol{x}}_{\boldsymbol{t}}^{(k)} \overleftarrow{\ }^{\forall t=1,2,\ldots,n_t} \begin{cases} \hat{J}_t^{(k)} = \underset{\boldsymbol{x_t}}{\text{Min}} \ \frac{1}{2}\left[\boldsymbol{z_t} - \boldsymbol{h_t}(\boldsymbol{x_t}, \boldsymbol{C}^{(k)})\right]^T \boldsymbol{R}_{\boldsymbol{z_t}}^{-1}\left[\boldsymbol{z_t} - \boldsymbol{h_t}(\boldsymbol{x_t}, \boldsymbol{C}^{(k)})\right] \\ \text{subject to} \\ \boldsymbol{l_t}(\boldsymbol{x_t}, \boldsymbol{C}^{(k)}) = \boldsymbol{0} \\ \boldsymbol{g_t}(\boldsymbol{x_t}, \boldsymbol{C}^{(k)}) \leq \boldsymbol{0} \end{cases}, \tag{4}$$

with (k) being an iteration counter. Note that for a given $\boldsymbol{C}^{(k)}$ the state estimation problem can be solved with a non-linear solver such as *CONOPT* (Drud, 1996) or *MINOS* (Murtagh and Saunders, 1998), which have proven to be robust and computationally efficient (Caro et al, 2008). Once the solution for subproblems $\hat{\boldsymbol{x}}_{\boldsymbol{t}}^{(\boldsymbol{k})}; \forall t = 1, 2, \ldots, n_t$ has been obtained, it is possible using sensitivity analysis to compute the derivatives of the objective function in (4) with respect to the roughness values $\boldsymbol{C}^{(k)}$, so that the original problem (1)-(3) can be approximated using the following master problem:

$$\underset{\boldsymbol{C}}{\text{Min}} \sum_{\forall t} \hat{J}_t^{(k)} + \sum_{\forall t} \frac{\partial \hat{J}_t^{(k)}}{\partial \boldsymbol{C}^{(k)}}(\boldsymbol{C} - \boldsymbol{C}^{(k)}) \tag{5}$$

Note that $\frac{\partial \hat{J}^{(k)}}{\partial \boldsymbol{C}^{(k)}} = \sum_{\forall t} \frac{\partial \hat{J}_t^{(k)}}{\partial \boldsymbol{C}^{(k)}}$, i.e. the sensitivity of the master problem can be obtained from the sensitivities of each of the subproblems. Such derivatives can be easily computed with any existing sensitivity analysis technique (see Piller et al (2017) for references).

It must be highlighted that decomposition techniques have traditionally been implemented as recursive procedures, i.e. firstly solving each of the subproblems, then computing the associated sensitivities and finally solving the master problem, to then repeat the process with a different parameter value (Conejo et al, 2006). However, in this work the computation of first-order derivatives is integrated within a quasi-Newton method to speed the process, as in such type of methods the Hessian can be approximated using gradient evaluations. More specifically, the Broyden-Fletcher-Goldfarb-Shanno (BFGS) quasi-Newton method (Broyden, 1970; Fletcher, 1970; Goldfarb, 1970; Shanno, 1970) with a cubic line search procedure is here adopted, as implemented in MatLab 7.12.0 (R2011a). Therefore, only an initial value $\boldsymbol{C}^{(0)}$ and a function that provides the value of J and $\frac{\partial J}{\partial \boldsymbol{C}}$ are required to run the calibration algorithm, which internally updates roughness coefficients as explained before.

It should be noted that the complexity of the calibration procedure increases as the number of pipe roughness coefficients (p) enlarges. In this regard, it is common practice to reduce the number of parameters by grouping pipes according to different criteria, such as age, material, diameter or relative location in the system (Kumar et al, 2010), and even work has been done to discuss the balance between the number of groups and model accuracy (Mallick et al, 2002). Grouping strategies are out of the scope of this work, but any of the already available techniques could be applied as a previous stage to calibration. Note that grouping pipes implies that the BFGS algorithm has to work with the derivatives of each objective function with respect to the group roughness $\boldsymbol{C_g}$ instead of the individual roughness of

each pipe $\boldsymbol{C}$, i.e. $\frac{\partial J^{(k)}}{\partial \boldsymbol{C}_{\boldsymbol{g}}^{(k)}} = \sum_{\forall t} \frac{\partial J_t^{(k)}}{\partial \boldsymbol{C}_{\boldsymbol{g}}^{(k)}}$ instead of $\frac{\partial J^{(k)}}{\partial \boldsymbol{C}^{(k)}} = \sum_{\forall t} \frac{\partial J_t^{(k)}}{\partial \boldsymbol{C}^{(k)}}$. At the same time, derivatives with respect to the group roughness can be computed by adding the derivatives of the pipes whose roughness values belong to the same group, i.e. $\frac{\partial J_t^{(k)}}{\partial \boldsymbol{C}_{\boldsymbol{g}}^{(k)}} = \sum_{\forall \boldsymbol{C} \in \boldsymbol{C_g}} \frac{\partial J_t^{(k)}}{\partial \boldsymbol{C^{(k)}}}$.

Finally, we want to highlight that this calibration approach takes full advantage of the available metering devices in any water distribution system, as it can be fed with the real-time information provided by telemetry systems at different times, e.g. at different times within a day or month, but at the same position. The use of multi-period data increases the robustness of the solution, as it takes into account very different flow scenarios that contribute to narrow down the unknown parameters. Therefore, the wide range of the data contributes to compensate the traditional scarcity of metering devices in water networks (Díaz et al, 2016) with the use of information over time. Moreover, the use of information over time enables the periodic reassessment of roughness values based on recent online measurements. This facilitates keeping an up-to-date model of the system, thus constituting a solid base on which other applications could be run. Note that the uncertainty of the estimated roughness coefficients could be obtained using sampling experiments (i.e. Monte Carlo method).

3 Observability analysis

The observability problem has been identified as one of the main difficulties associated with the calibration process (Piller, 1995; Kumar et al, 2010), and is considered a prior essential step when implementing calibration strategies at an operational level, either considering static, quasi-static or dynamic models (Pérez, 2003). Moreover, observability analysis for state estimation has been a topic of extensive research in both the water and power supply fields (see Díaz et al (2016) for references). For this reason, it is a matter of interest to develop a consistent methodology that enables to assess the system observability and identify the observable model parameters for a given measurement setting when implementing the aforementioned calibration procedure.

In this section, observability analysis is adapted for the novel calibration methodology presented in this paper. Firstly, guidelines are given to build the associated measurement and parameter Jacobian matrix. Then, an already available in the literature methodology is selected to analyse the observability of the problem.

3.1 Measurement and parameter Jacobian matrix

In a conventional single-period state estimation application, the measurement Jacobian matrix $\boldsymbol{H} \in \mathbb{R}^{m \times n}$ contains the first-order partial derivatives of all the possible measurements within the system (i.e. flow, water level, pressure or demand measurements) with respect to all the state variables (i.e. head levels) at that time. This matrix contains all the information about the system's flow governing equations, thus a theoretical and sufficient condition for the state estimation problem to have a unique so-

lution is that matrix $\boldsymbol{H}$ has full rank n, with $m \geq n$ (Díaz et al, 2016a). In order to assess the observability of the novel calibration procedure, a multi-period measurement and parameter Jacobian matrix needs to be similarly built $\boldsymbol{M} \in \mathbb{R}^{(m \times n_t) \times (n \times n_t + p)}$. Note that even though the original joint parameter and state estimation problem is decomposed for calibration purposes, both head levels and model parameters have to be observable to enable the solution of the subproblems and the master problem at different stages. Therefore, the observability of the combined parameter and state estimation problem (1)-(3) has to be analysed.

Figure 1 shows the structure of the resulting multi-period measurement and parameter Jacobian matrix. As mentioned before, in this case there are $n \times n_t + p$ state variables, which are introduced in the matrix as columns, and $m \times n_t$ measurements, which appear in the matrix as rows. Accordingly, the measurement Jacobian matrix for each time ($\boldsymbol{H_t}; \forall t = 1, 2, \ldots, n_t$) must be introduced in the multi-period Jacobian matrix, whose size considerably increases with the number of time steps taken into consideration for calibration purposes. A detailed description of how to build the measurement Jacobian matrix for each time is provided in Díaz et al (2016). Additionally, the derivatives of each of the measurements with respect to roughness coefficients must be considered for the analysis, i.e. the roughness Jacobian matrix $\boldsymbol{P} \in \mathbb{R}^{m \times p}$ must be built. As roughness values are considered constant over time, the sum of the derivatives at each time ($\boldsymbol{P_t}; \forall t = 1, 2, \ldots, n_t$) should be included in the combined matrix.

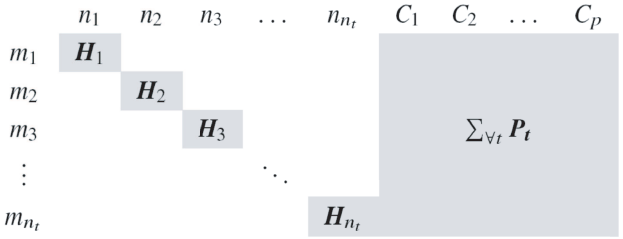

Fig. 1 Structure of the multi-period measurement and parameter Jacobian matrix $\boldsymbol{M}$

Note that the $\boldsymbol{M}$ matrix must be computed for a specific flow scenario, but an iterative evaluation for each of the $\boldsymbol{C}^{(k)}$ or $\boldsymbol{C_g}^{(k)}$ values considered along the process would be time-consuming. For this reason, it is recommended to build the joint Jacobian matrix with an approximate estimate of the roughness values that are to be calibrated. This provides a good insight of the system observability, but could lead to inconsistent results if the estimate is far from the assumed value. Nevertheless, as this calibration procedure is conceived to be periodically repeated in networks gifted with telemetry systems, the initial value could be taken as the last estimated roughness, thus ensuring a reasonable approximation to the next value.

3.2 Algorithm for observability analysis

Once the multi-period measurement and parameter Jacobian matrix has been built, any method for observability analysis can be implemented. As commented by Díaz et al (2017), such analysis can be undertaken evaluating the rank of the matrix constituted by only the available measurements over time, or considering the full Jacobian matrix. Note that the second approach enables to assess the observability of all variables within the system rather than only the state variables. As the ultimate objective of the methodology developed in this paper is to calibrate model parameters, and roughness coefficients are included as state variables, the first type of methods can be used. Note that such choice enables to work with a $(m \times n_t) \times (n \times n_t + p)$ matrix, whose size can already be considerable for large systems when using a significant number of time steps.

More specifically, the null-space method proposed by Castillo et al (2005) is used in this work. According to this approach, the system is fully observable when the null-space matrix of the Jacobian is an empty set, and unobservable when it is not. As the general solution of any system of equations can be written in terms of a particular solution and the scalar product of the null-space matrix ($\boldsymbol{N} \in \mathbb{R}^{(n \times n_t + p) \times k}$) and an arbitrary k-dimensional vector, the method also permits to identify observable elements even when the system is unobservable in the overall. Those state variables that present zero-rows in the null-space matrix can be determined with only their particular solution, thus they are observable. In order to avoid numerical problems, which may happen since $\boldsymbol{M}$ is prone to ill-conditioning due to the difference in order of magnitude between the components of $\boldsymbol{H_t}; \forall t = 1, 2, \ldots, n_t$ and $\boldsymbol{P_t}; \forall t = 1, 2, \ldots, n_t$, the null-space of the normalised matrix $\boldsymbol{M}$ should be computed. Note that the normalised matrix can be obtained by simply dividing all the components of each row by the maximum absolute value in that row. Moreover, Singular Value Decomposition (SVD) is recommended to systematically compute the null-space and is used in this work all along.

4 Case study

The Hanoi network as presented by Díaz et al (2016a) is adopted as case study in this paper. Figure 2 provides the network layout, where 1 source node provides water to 31 junctions through 34 pipes. Such benchmark network is only modified here in terms of pipe roughness coefficients. As grouping techniques are out of the scope of this paper, pipes are grouped in three different ways in this work just for the sake of showing how the performance of the algorithm is affected by the number of roughness coefficients considered for calibration. Figure 3 provides the three associations that are assumed along the case study, together with the real value of the roughness coefficient for each group ($\boldsymbol{C_{g,real}}$), which is required to artificially generate measurements.

In what regards measurement configurations, several scenarios are used for calibration in this case study. In all of them, the water level at the source tank and water demands at all nodes are metered (base scenario), as if the Hanoi system was a water

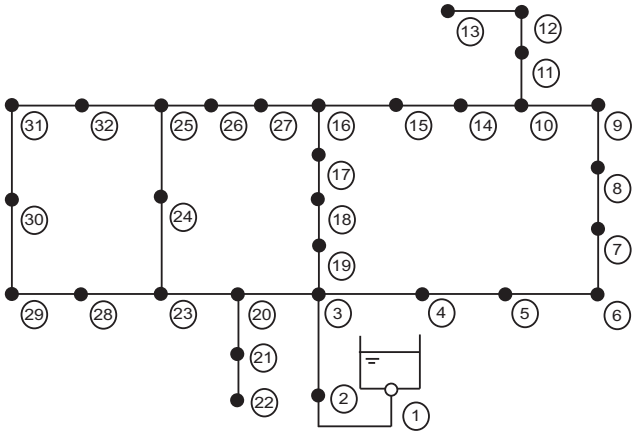

Fig. 2 Layout of Hanoi network case study

transport network in which all outflows are monitored. Note that such measurement configuration would ensure the system observability if conventional state estimation was undertaken, i.e. if only head levels had to be computed at each time step. Nevertheless, as roughness coefficients must be adjusted, additional meters are included in this case study. Five measurement scenarios are here tested: (a) 1 level of redundancy, (b) 2 levels of redundancy, (c) 3 levels of redundancy, (d) 5 levels of redundancy, and (e) all hydraulic variables are metered. Note that the level of redundancy refers to the number of extra measurements with respect to the aforementioned base scenario, in which only the water level at the source tank and water demands at all nodes are metered. Table 1 gives the measurement setting associated with each of such scenarios. For example, scenario a) includes one extra pressure measurement at node 30 (1 level of redundancy), and scenario b) includes two extra pressure meters at nodes 30 and 9 (2 levels of redundancy). In terms of the noise to which those measurements are subjected, two versions are here simulated: exact measurements or measurements not subjected to noise ("E"), and noisy measurements ("N"), where pressure meters are subjected to a deviation $\sigma_x = 0.01$ bar and flow meters and demand meters are affected by $\sigma_Q = \sigma_q = 0.25$ m^3/h. Moreover, as the proposed calibration procedure is conceived to use available online measurements over time, 24 measurement configurations are considered in this paper for all the aforementioned scenarios, one at each hour during a full day. The base demand for the Hanoi network case study is modified at each hour by demand factors given in Figure 4. As this figure shows, the minimum demand is registered at 4-5h and represents 35% of the base demand of the network, and the peak consumption takes place at 13h, multiplying the base demand by 2. Therefore, in exact measurement scenarios, metered values exactly correspond to the solution of the flow network according to such consumptions, whereas in noisy configurations, metered values are perturbed around each flow network solution.

Calibration results considering two, three and five groups of pipes are shown hereafter. In each of such pipe configurations, both observability analysis and calibration results for all five measurement scenarios without and with noise measurements are

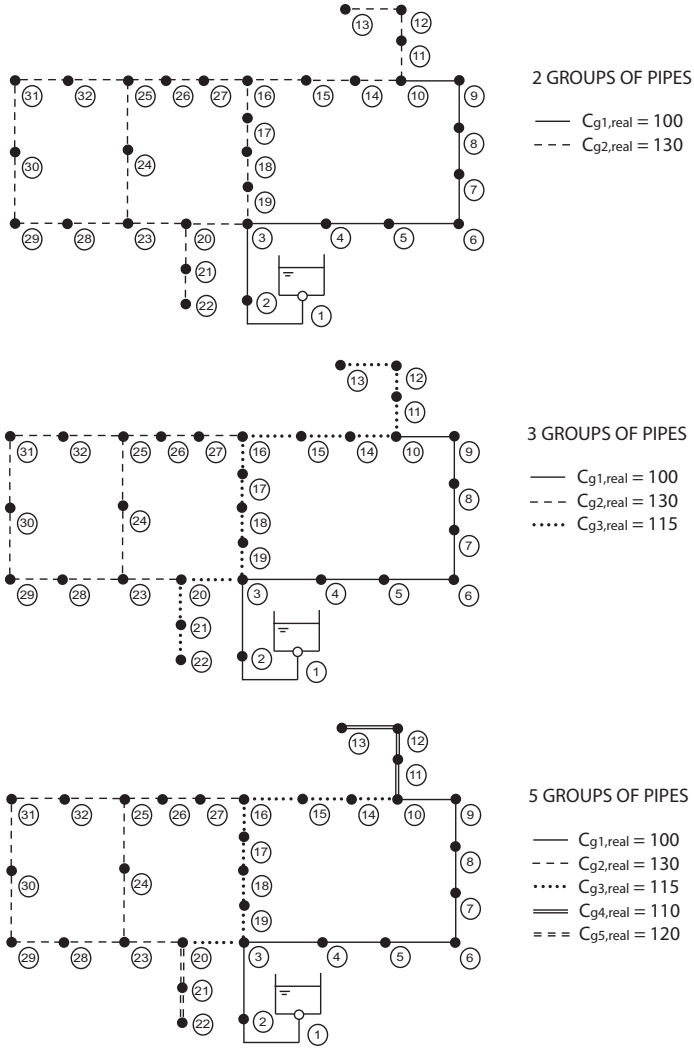

Fig. 3 Group roughness values considered for Hanoi network case study

Table 1 Measurement scenarios for Hanoi network case study

Measurement scenario	Level of redundancy	Pressure meters	Flow meters	Demand meters
a	1	Node 1, 30	-	All nodes
b	2	Nodes 1, 30, 9	-	All nodes
c	3	Nodes 1, 30, 9, 4	-	All nodes
d	5	Nodes 1, 30, 9, 4, 24	Pipe 2-3	All nodes
e	All	All nodes	All pipes	All nodes

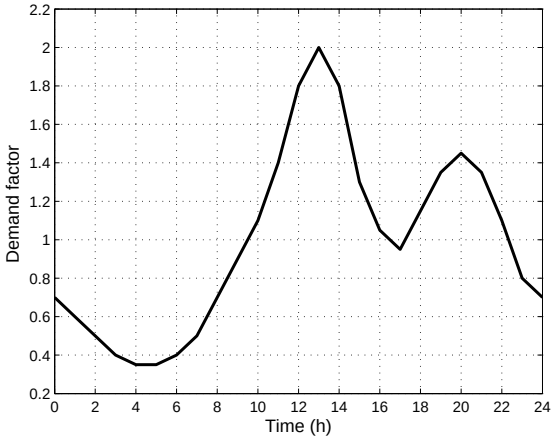

Fig. 4 Demand factors over time for Hanoi network case study

provided and discussed. All computations have been carried out in a MatLab 7.12.0 (R2011a) 64-bits version and a 23.3 GAMS 64-bits version, both run in an Intel(R) Core(TM) i7-6700 CPU 3.40 GHz 16 GB RAM desktop computer.

4.1 Two groups of pipes

To start with, Table 2 provides both observability analysis and calibration results for all exact measurement scenarios when two groups of pipes exist in the network, i.e. when only two roughness coefficients are to be calibrated. Beginning with observability analysis (OA), which in this work is analysed considering $\boldsymbol{C_{g,real}}$ values, the second column of this table shows that with one level of redundancy (scenario 2aE) the system is not observable. In fact, none of the roughness coefficients is observable for such measurement scenario, but the full system observability is ensured for the rest of measurement settings. In the next column, the value of the objective function of the calibration problem is provided for $\boldsymbol{C_{g,real}}$ values (J_{real}). As Table 2 corresponds to error free-measurements, such value is approximately zero for all cases (negative values are explained by the specified zero-tolerance). Then, calibration results are provided for two initial values $\boldsymbol{C_g^{(0)}}$. Two starting points have been considered all along this case study with the aim of showing how the BFGS algorithm performance is affected by the initial value. For each of such solutions, optimal roughness coefficients ($\hat{\boldsymbol{C}}_{\boldsymbol{g}}$), the value of the objective function at the optimum ($\hat{J}$), the number of objective function evaluations needed to reach the optimum (n_e), and the time required for the BFGS algorithm to converge in a desktop computer (t_c) are provided. As this table shows, the method converges to the correct roughness values in scenarios 2bE, 2cE, 2dE and 2eE no matter the starting point. Nevertheless, the calibration process converges to different values in scenario 2aE, which implies that no unique solution exists to the calibration process, as it depends on the initial value.

Such result proves the importance of observability analysis, as this prior step permits to know beforehand that roughness coefficients cannot be uniquely adjusted for this measurement setting, without the need of running the calibration algorithm itself. On the other hand, the objective function $\hat{J}$ is approximately zero for all error-free scenarios regardless of the starting point, and the number of function evaluations, which is directly related to the convergence time, does not seem to significantly increase when starting further from the optimum. Note that the computational time required to adjust roughness parameters in all scenarios remains lower than 8 minutes.

Table 2 Observability analysis and calibration results: exact measurements for two groups of pipes

			From $\boldsymbol{C_g^{(0)}} = [90; 117]$				From $\boldsymbol{C_g^{(0)}} = [90; 90]$			
Case*	OA	J_{real}	$\hat{\boldsymbol{C}}_{\boldsymbol{g}}$	$\hat{J}$	n_e	t_c (s)	$\hat{\boldsymbol{C}}_{\boldsymbol{g}}$	$\hat{J}$	n_e	t_c (s)
2aE	Unobs	5.6811e-8	102.9127	4.2142e-8	8	165.3343	112.2342	-2.1420e-8	9	200.2739
			122.4294				105.1343			
2bE	Obs	6.7521e-8	100.0000	2.3516e-8	15	297.1207	100.0000	6.2864e-8	14	301.6791
			130.0000				130.0001			
2cE	Obs	8.8476e-9	100.0000	7.9162e-9	15	301.3898	100.0000	4.9360e-8	14	285.0134
			130.0000				130.0000			
2dE	Obs	3.9041e-6	100.0000	4.1798e-6	14	323.2315	100.0000	3.7029e-6	14	338.6271
			130.0000				130.0000			
2eE	Obs	1.8328e-6	100.0000	-6.2585e-7	12	235.1822	100.0000	2.8759e-6	19	421.1136
			130.0000				129.9999			

*2 refers to the number of roughness coefficients or pipe groups considered for calibration (as described in Figure 3); letters a-e refer to the measurement configuration (as described in Table 1); and "E" implies that measurements are exact (i.e. not subjected to noise)

Table 3 provides the same results for noisy measurement scenarios. As this table shows, the system remains unobservable for setting 2aN (i.e. $\hat{\boldsymbol{C}}_{\boldsymbol{g}}$ values are different for the two initialisations) and observability is still ensured for the rest of the cases. In what regards J_{real}, the objective function for $\boldsymbol{C_{g,real}}$ is now different from zero in all cases, and increases with the level of redundancy. This is explained by the fact that measurements are subjected to noise, thus the $\boldsymbol{C_g}$ values that better adjust to the measurement setting are no longer $\boldsymbol{C_{g,real}} = [100; 130]$, but slightly different. Note that such deviation is due to the fact that only 24 noisy measurements are considered for calibration, but a better adjustment would be obtained if more online measurements were incorporated. As $\hat{\boldsymbol{C}}_{\boldsymbol{g}}$ better fits the noisy measurements, $\hat{J}$ is smaller than J_{real} for all case scenarios. The speed of convergence seems to be very similar for both $\boldsymbol{C_g^{(0)}}$ values.

Finally, Figure 5 provides contour maps of how the objective function changes with $\boldsymbol{C_g}$ for the observable cases (2bE, 2cE, 2dE, 2eE, 2bN, 2cN, 2dN and 2eN). Starting with case 2bE (i.e. two levels of redundancy and measurements not subjected to noise), the figure shows that the objective function of the multi-period calibration problem is convex, with the minimum located at $\hat{\boldsymbol{C}}_{\boldsymbol{g}} = \boldsymbol{C_{g,real}} = [100; 130]$. This

Table 3 Observability analysis and calibration results: noisy measurements for two groups of pipes

			From $\boldsymbol{C_g^{(0)}} = [90; 117]$				From $\boldsymbol{C_g^{(0)}} = [90; 90]$			
Case*	OA	J_{real}	$\hat{\boldsymbol{C}}_{\boldsymbol{g}}$	$\hat{J}$	n_e	t_c (s)	$\hat{\boldsymbol{C}}_{\boldsymbol{g}}$	$\hat{J}$	n_e	t_c (s)
2aN	Unobs	13.3775	102.9414	11.9807	8	176.1451	112.2905	12.0318	9	217.6179
			122.4474				105.1190			
2bN	Obs	23.6220	100.0042	23.5668	15	328.3052	100.0042	23.5668	14	314.8889
			129.9792				129.9792			
2cN	Obs	29.1701	99.9752	27.6410	14	466.9487	99.9752	27.6410	13	289.0662
			130.0600				130.0601			
2dN	Obs	61.0293	99.9888	60.7363	14	449.5603	99.9888	60.7363	13	310.0673
			130.0186				130.0186			
2eN	Obs	774.5133	100.0108	773.2475	13	346.4825	100.0108	773.2475	17	407.0368
			130.0144				130.0144			

*2 refers to the number of roughness coefficients or pipe groups considered for calibration (as described in Figure 3); letters a-e refer to the measurement configuration (as described in Table 1); and "N" implies that measurements are noisy

figure also shows that the change in the objective function is more evident in the horizontal direction, i.e. the objective function is more sensitive to C_{g1} than to C_{g2}. Therefore, we can conclude that parameter C_{g1} is more identifiable, which is consistent with the reality of the network because the pipes that correspond to such group (see Figure 3) are located at the right-hand side of the system and are associated with greater flows, thus they can be more easily adjusted based on sensitivity analysis. Also, Figure 5 shows that the objective function becomes more convex as the number of metering devices increases, because contour lines associated with cases 2cE and 2dE are closer to the optimum value than in case 2bE. Nevertheless, there is a change in pattern for case 2eE: as in this scenario all hydraulic variables are metered, contour lines have a slope close to 45, which implies that the sensitivity to C_{g1} and C_{g2} is very similar. Note that in this case the objective function reaches much higher values, which indicates that the function has considerably convexified around the optimum. On the other hand, contour maps of cases 2bN, 2cN, 2dN and 2eN (right side of the figure) are very similar to their equivalents without noise (in the left), with the only difference being that the objective function presents now higher values as a result of the noise consideration (i.e. the objective function is vertically displaced), and that the optimum value has slightly moved from $\boldsymbol{C_{g,real}}$.

4.2 Three groups of pipes

Tables 4 and 5 provide observability analysis and calibration results for exact and noisy measurement scenarios when considering that three groups of pipes exist in Hanoi network, i.e. three roughness coefficients are to be calibrated. In this case, the system results unobservable (with all three $\boldsymbol{C_g}$ values being unobservable) for measurement settings 3aE, 3aN, 3bE and 3bN, i.e. when only one or two levels of

redundancy exist. For such cases, the BFGS algorithm converges to different values when starting from different starting points, but for the rest of observable scenarios, the same solution is reached no matter the initialisation. As before, optimal values are close to $\boldsymbol{C_{g,real}}$ for the without-noise scenarios, but differ slightly when noise is taken into account. The convergence time and number of function evaluations has increased with respect to the previous section as a result of the increase in the number of parameters, but it is still reasonable and similar regardless of the initialisation.

Table 4 Observability analysis and calibration results: exact measurements for three groups of pipes

			From $\boldsymbol{C_g^{(0)}} = [90; 117; 103.5]$				From $\boldsymbol{C_g^{(0)}} = [90; 90; 90]$			
Case*	OA	J_{real}	$\hat{\boldsymbol{C}}_{\boldsymbol{g}}$	$\hat{J}$	n_e	t_c (s)	$\hat{\boldsymbol{C}}_{\boldsymbol{g}}$	$\hat{J}$	n_e	t_c (s)
3aE	Unobs	2.4913e-8	103.9502	3.5856e-8	8	163.1314	113.7080	-2.1653e-8	9	193.2424
			120.7061				100.4243			
			106.6725				98.1217			
3bE	Unobs	3.6554e-8	100.2048	-8.1491e-9	15	322.5363	99.9644	1.4436e-8	15	322.3756
			131.6885				129.7138			
			112.0086				115.5316			
3cE	Obs	4.6333e-8	100.0000	1.9325e-8	26	542.2622	100.0009	1.3642e-5	21	443.5707
			130.0000				130.0114			
			115.0000				114.9838			
3dE	Obs	7.8976e-6	100.0000	7.5921e-6	25	627.2670	100.0000	7.7486e-6	25	616.1586
			129.9998				130.0000			
			115.0003				115.0000			
3eE	Obs	5.6967e-5	99.9999	5.7295e-5	27	549.8109	100.0000	5.8636e-5	24	1.1874e+3
			129.9999				130.0000			
			114.9999				115.0000			

*3 refers to the number of roughness coefficients or pipe groups considered for calibration (as described in Figure 3); letters a-e refer to the measurement configuration (as described in Table 1); and "E" implies that measurements are exact (i.e. not subjected to noise)

4.3 Five groups of pipes

Tables 6 and 7 provide the same results when five groups of pipes are distinguished, i.e. when five roughness parameters are to be calibrated. In this case, the system is only observable for scenarios 5eE and 5eN among the examples tested. This fact must be highlighted because in the previous sections, two and three levels of redundancy were enough to guarantee the system observability when two and three roughness groups existed, but in this case five levels of redundancy (scenarios 5dE and 5dN) are not sufficient to adjust five roughness values. However, some of the roughness parameters are observable regardless of the system's lack of observability. The application of the null-space method indicates that even though the system in the overall

Table 5 Observability analysis and calibration results: noisy measurements for three groups of pipes

			From $\boldsymbol{C_g^{(0)}} = [90; 117; 103.5]$				From $\boldsymbol{C_g^{(0)}} = [90; 90; 90]$			
Case*	OA	J_{real}	$\hat{\boldsymbol{C}}_{\boldsymbol{g}}$	$\hat{J}$	n_e	t_c (s)	$\hat{\boldsymbol{C}}_{\boldsymbol{g}}$	$\hat{J}$	n_e	t_c (s)
3aN	Unobs	13.3986	103.9812	11.9979	8	186.9955	113.7666	12.0535	9	212.2409
			120.7186				100.3643			
			106.6834				98.1712			
3bN	Unobs	23.6075	100.2084	23.5453	15	333.1195	99.9629	23.5497	15	346.6269
			131.6632				129.6489			
			112.0010				115.5996			
3cN	Obs	29.1712	99.9646	27.4212	26	611.6861	99.9646	27.4212	22	533.4064
			129.9061				129.9061			
			115.2627				115.2625			
3dN	Obs	61.0049	99.9853	60.6888	25	611.7809	99.9854	60.6888	25	617.8526
			129.9586				129.9587			
			115.0894				115.0891			
3eN	Obs	773.6400	100.0102	771.8931	17	359.3844	100.0102	771.8931	22	1.1242e+3
			130.0112				130.0112			
			115.0125				115.0125			

*3 refers to the number of roughness coefficients or pipe groups considered for calibration (as described in Figure 3); letters a-e refer to the measurement configuration (as described in Table 1); and "N" implies that measurements are noisy

is not observable, C_{g1}, C_{g2} and C_{g3} are observable in cases 5cE, 5dE, 5cN and 5dN (i.e. when three and five levels of redundancy exist), which matches results shown in Tables 6 and 7. Such a solution is consistent with the reality of the network, because groups C_{g4} and C_{g5} are formed by the two branches that come out of the main looped structure (see Figure 3). As these branches are subjected to low flow, they are expected to have low identifiability and be difficult to adjust when low redundancy exists. Note that results from Tables 4 and 6 are very similar to each other, and so are those in Tables 5 and 7, except for the new groups incorporated. Additionally, the number of function evaluations (i.e. convergence time) is in this case very similar to that obtained when only considering three groups. This may lead to think that as long as some of the roughness values are observable, the algorithm could be applied to the system in order to obtain as much information as possible without burdening the convergence speed.Note that the associated computational time remains in all cases below 30 minutes, which is reasonable for such an application in a medium size water system.

5 Conclusions

In this work, the calibration problem is conceived as a joint parameter and state estimation problem, which is then decomposed to leave model parameters (i.e. roughness coefficients) as the only variables. As many other approaches in the technical liter-

Table 6 Observability analysis and calibration results: exact measurements for five groups of pipes

			From $\boldsymbol{C}_{\boldsymbol{g}}^{(0)} = [90; 117; 103.5; 99; 108]$				From $\boldsymbol{C}_{\boldsymbol{g}}^{(0)} = [90; 90; 90; 90; 90]$			
Case*	OA	J_{real}	$\hat{\boldsymbol{C}}_{\boldsymbol{g}}$	$\hat{J}$	n_e	t_c (s)	$\hat{\boldsymbol{C}}_{\boldsymbol{g}}$	$\hat{J}$	n_e	t_c (s)
5aE	Unobs	3.7253e-9	103.9502	4.0280e-8	8	164.7195	113.7080	2.3982e-8	9	196.9345
			120.7061				100.4243			
			106.6725				98.1217			
			99.0000				90.0000			
			108.0000				90.0000			
5bE	Unobs	-1.0000e-15	100.2048	-1.7229e-8	15	316.8454	99.9644	-5.8208e-9	15	313.5507
			131.6885				129.7138			
			112.0086				115.5316			
			99.0000				90.0000			
			108.0000				90.0000			
5cE	Unobs	2.4447e-8	100.0000	-1.3504e-8	26	540.8685	100.0009	1.3630e-5	21	452.7968
			130.0000				130.0114			
			115.0000				114.9838			
			99.0000				90.0000			
			108.0000				90.0000			
5dE	Unobs	7.6964e-6	100.0000	9.0525e-6	25	651.4509	100.0001	1.1072e-5	26	621.7441
			129.9998				130.0002			
			115.0003				114.9997			
			99.0000				90.0000			
			108.0000				90.0000			
5eE	Obs	6.4641e-5	100.0000	6.2987e-5	45	947.2427	99.9994	0.0025	47	1.3760e+3
			130.0000				129.9992			
			115.0000				114.9993			
			110.0000				110.0573			
			120.0000				120.0019			

*5 refers to the number of roughness coefficients or pipe groups considered for calibration (as described in Figure 3); letters a-e refer to the measurement configuration (as described in Table 1); and "E" implies that measurements are exact (i.e. not subjected to noise)

ature, the proposed method is conceived as a multi-period analysis, which enables consideration of different flow conditions to better adjust unknown model parameters. Nevertheless, the methodology presented in this paper is different from conventional calibration strategies, as it considers that all measurements can be subjected to noise thanks to its state estimation structure. This enables the use of first-hand real-time information provided by SCADA systems for calibration purposes.

Also, a methodology to assess the observability of such a problem is presented. The method permits to identify the roughness coefficients that can be calibrated based on the available measurement setting, thus enabling to save time when measurements are not sufficient. This is of special interest nowadays, because even though the installation of new devices is on its way, many water distribution systems are still limited in

Table 7 Observability analysis and calibration results: noisy measurements for five groups of pipes

			From $\boldsymbol{C_g^{(0)}} = [90; 117; 103.5; 99; 108]$				From $\boldsymbol{C_g^{(0)}} = [90; 90; 90; 90; 90]$			
Case*	OA	J_{real}	$\hat{\boldsymbol{C}}_{\boldsymbol{g}}$	$\hat{J}$	n_e	t_c (s)	$\hat{\boldsymbol{C}}_{\boldsymbol{g}}$	$\hat{J}$	n_e	t_c (s)
5aN	Unobs	13.3986	103.9812	11.9979	8	179.4745	113.7666	12.0535	9	211.7089
			120.7186				100.3643			
			106.6834				98.1712			
			99.0000				90.0000			
			108.0000				90.0000			
5bN	Unobs	23.6075	100.2084	23.5453	15	335.2300	99.9629	23.5497	15	344.1667
			131.6632				129.6489			
			112.0010				115.5996			
			99.0000				90.0000			
			108.0000				90.0000			
5cN	Unobs	29.1712	99.9646	27.4212	26	609.4641	99.9646	27.4212	22	527.3345
			129.9061				129.9061			
			115.2627				115.2625			
			99.0000				90.0000			
			108.0000				90.0000			
5dN	Unobs	61.0049	99.9853	60.6888	25	603.4838	99.9854	60.6888	25	611.7869
			129.9586				129.9587			
			115.0894				115.0891			
			99.0000				90.0000			
			108.0000				90.0000			
5eN	Obs	773.6378	100.0105	771.6431	40	860.4153	100.0103	771.6437	43	1.7798e+3
			130.0115				130.0112			
			115.0129				115.0126			
			110.0119				110.0133			
			119.9828				119.9831			

*5 refers to the number of roughness coefficients or pipe groups considered for calibration (as described in Figure 3); letters a-e refer to the measurement configuration (as described in Table 1); and "N" implies that measurements are noisy

terms of instrumentation, and some measurements can occasionally fail (e.g. sensor failure, communication failure). Note that observability analysis enables identification of networks that cannot be calibrated with available measurements, but it also sets up a basis on which sampling design strategies could be developed. This is a subject for further research.

Results highlight the robustness of the observability-calibration tool presented in this paper, which has proven to work effectively for both exact and noisy measurements in the considered case study. Moreover, convergence time is not severely affected by the distance between the initialisation and the optimum, mainly thanks to the use of sensitivity analysis to iteratively update model parameters. This fact is of special interest in real-life networks, where a good initialisation may not be possible

due to the lack of periodic calibration. Note that if unrealistic roughness values are obtained for observable parameters, this would constitute an indicator of abnormal conditions in such pipes, i.e. a change in the pump and valve setting, a burst, etc. Therefore, the proposed novel methodology not only contributes to keeping an up-to-date model of the system, but also furthers the knowledge on the network's real-time behavior, thus contributing to taking full advantage of available telemetry systems.

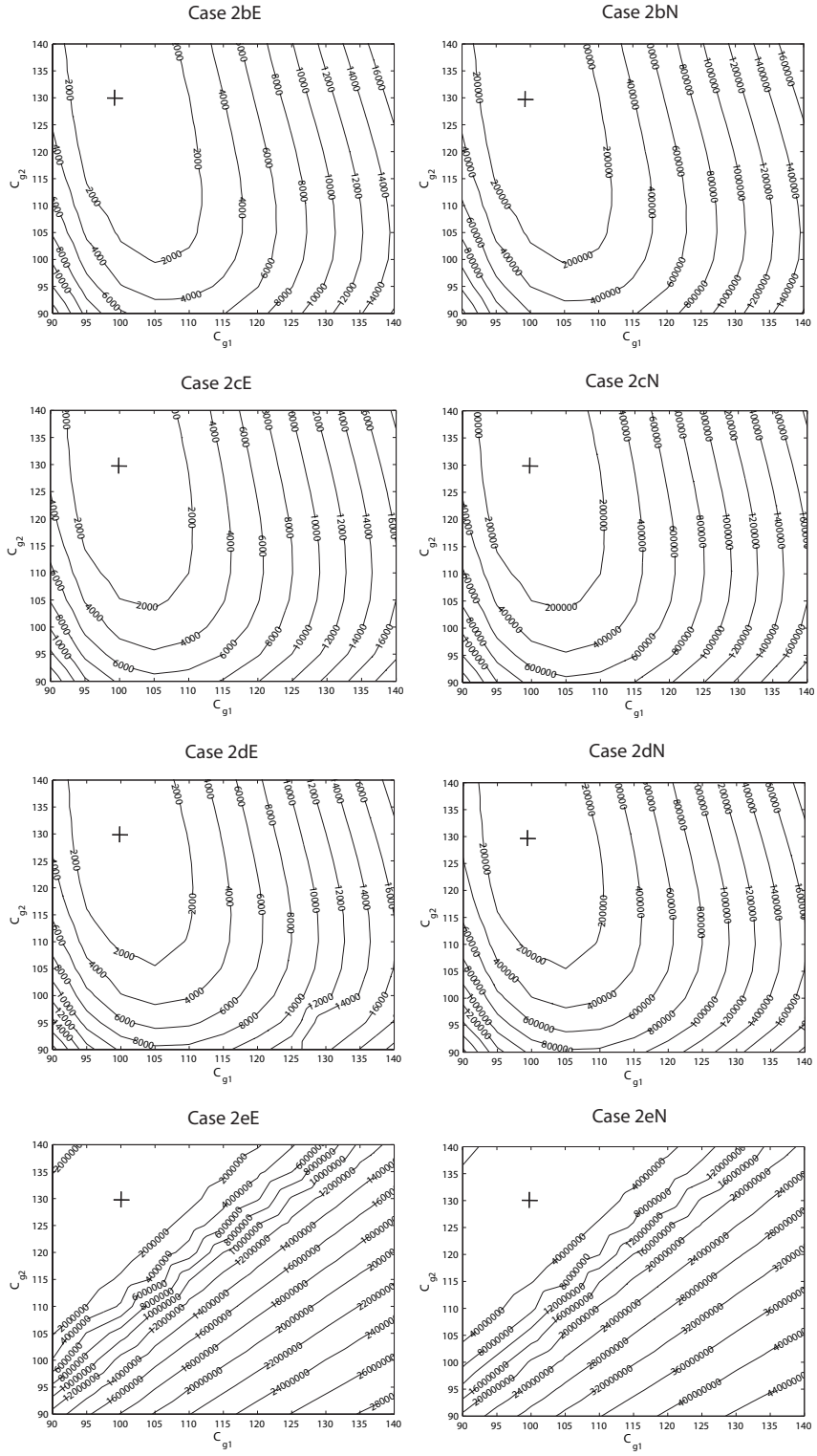

Fig. 5 Contour maps of the objective function for observable cases*: two groups of pipes
*2 refers to the number of roughness coefficients or pipe groups considered for calibration (as described in Figure 3); letters b-e refer to the measurement configuration (as described in Table 1); "E" implies that measurements are exact (i.e. not subjected to noise) and "N" implies that measurements are noisy

References

Bhave PR (1988) Calibrating water distribution network models. J Environ Eng 114(1):120–136

Boulos PF, Ormsbee LE (1991) Explicit network calibration for multiple loading conditions. Civ Eng Syst 8(3):153–160

Boulos PF, Wood DJ (1990) Explicit calculation of pipe-network parameters. J Hydraul Eng 116(11):1329–1344

Brdys MA, Chen K (1993) Joint state and parameter estimation of dynamic water supply systems with unknown but bounded uncertainty. In: Coulbeck B (ed) Integrated Computer Applications in Water Supply, vol 1, Research Studies Press, Baldock, UK, pp 335–355

Brdys MA, Chen K (1994) Joint state and parameter estimation of dynamic water supply system under bounded uncertainty using geometric programming. In: Blanke M, Soderstrom T (eds) Proceedings 10 IFAC Symposium on System Identification, vol 3, Copenhaguen, Denmark, pp 331–336

Brdys MA, Ulanicki B (2002) Operational control of water systems: Structures, algorithms and applications. Prentice Hall, London, UK

Broyden CG (1970) The convergence of a class of double-rank minimization algorithms: 2. The new algorithm. J Inst Math Appl 6(3):222–231

Caro E, Conejo AJ, Mínguez R (2008) A mathematical programming approach to state estimation. In: Castronuovo ED (ed) Optimization Advances in Electric Power Systems, Nova Science Publishers, New York, USA, pp 1–26

Castillo E, Conejo AJ, Pruneda RE, Solares C (2005) State estimation observability based on the null space of the measurement jacobian matrix. IEEE Trans Power Syst 20(3):1656–1658

Conejo AJ, Castillo E, Mínguez R, García-Bertrand R (2006) Decomposition techniques in mathematical programming. Engineering and science applications. Springer-Verlag Berlin Heidelberg, New York, USA

Datta RSN, Sridharan K (1994) Parameter estimation in water-distribution systems by least squares. J Water Resour Plann Manage 120(4):405–422

Díaz S, González J, Mínguez R (2016) Observability analysis in water transport networks: Algebraic approach. J Water Resour Plann Manage 142(4):04015071, DOI 10.1061/(ASCE)WR.1943-5452.0000621

Díaz S, González J, Mínguez R (2016a) Uncertainty evaluation for constrained state estimation in water distribution systems. J Water Resour Plann Manage 142(12):06016004, DOI 10.1061/(ASCE)WR.1943-5452.0000718

Díaz S, Mínguez R, González J (2017) Topological observability analysis in water distribution systems. J Water Resour Plann Manage 143(5):06017001, DOI 10.1061/(ASCE)WR.1943-5452.0000762

Drud A (1996) CONOPT: A system for large scale nonlinear optimization. ARKI Consulting and Development A/S, Bagsvaerd, Denmark

Fletcher R (1970) A new approach to variable metric algorithms. Comput J 13(3):317–322

Goldfarb D (1970) A family of variable-metric methods derived by variational means. Math Comput 24(109):23–26

Kapelan ZS, Savic DA, Walters GA (2007) Calibration of water distribution hydraulic models using a bayesian-type procedure. J Hydraul Eng 133(8):927–936

Kumar SM, Narasimhan S, Bhallamudi SM (2008) State estimation in water distribution networks using graph-theoretic reduction strategy. J Water Resour Plann Manage 134(5):395–403

Kumar SM, Narasimhan S, Bhallamudi SM (2010) Parameter estimation in water distribution networks. Water Resour Manage 24(6):1251–1272

Lansey KE, Basnet C (1991) Parameter estimation for water distribution networks. J Water Resour Plann Manage 117(1):126–144

Lansey KE, El-Shorbagy W, Ahmed I, Araujo J, Haan CT (2001) Calibration assessment and data collection for water distribution networks. J Hydraul Eng 127(4):270–279

Mallick KN, Ahmed I, Tickle KS, Lansey KE (2002) Determining pipe groupings for water distribution networks. J Water Resour Plann Manage 128(2):130–139

Murtagh BA, Saunders MA (1998) MINOS 5.5 user's guide. Rep SOL 83-20R, Dept of Operations Research, Stanford Univ, USA

Pérez R (2003) Identifiability and calibration of water network models. PhD thesis, Univ. Politécnica de Catalunya, Spain

Piller O (1995) Modeling the behavior of a network - hydraulic analysis and sampling procedures for parameter estimation. PhD thesis, Univ. of Bordeaux, France

Piller O, Elhay S, Deuerlein J, Simpson AR (2017) Local sensitivity of pressure-driven modeling and demand-driven modeling steady-state solutions to variations in parameters. J Water Resour Plann Manage 143(2):04016074

Rahal CM, Sterling MJH, Coulbeck B (1980) Parameter tuning for simulation models of water distribution networks. Proc Inst Civ Eng 69(3):751–762

Reddy PVN, Sridharan K, Rao PV (1996) WLS method for parameter estimation in water distribution networks. J Water Resour Plann Manage 122(3):157–164

Savic DA, Walters GA (1995) Genetic algorithm techniques for calibrating network models. Tech. Rep. 95/12, Centre for Systems and Control Engineering, Univ. of Exeter, UK

Savic DA, Kapelan ZS, Jonkergouw PMR (2009) Quo vadis water distribution model calibration? Urban Water J 6(1):3–22

Shanno DF (1970) Conditioning of quasi-newton methods for function minimization. Math Comput 24(111):647–656

Wu ZY, Clark C (2009) Evolving effective hydraulic model for municipal water systems. Water Resour Manage 23(1):117–136